Title	Flexible and semi-transparent chipless RFID tag based on PDMS-conductive fabric composite
Authors	Rather, Nadeem;Simorangkir, Roy B. V. B.;Buckley, John;O'Flynn, Brendan
Publication date	2022-07-04
Original Citation	Rather, N., Simorangkir, R. B. V. B., Buckley, J. and O'Flynn, B. (2022) 'Flexible and semi-transparent chipless RFID tag based on PDMS-conductive fabric composite', 2022 International Workshop on Antenna Technology (iWAT), Dublin, Ireland, 16-18 May, pp 33-36. https://doi.org/10.1109/iWAT54881.2022.9811001
Type of publication	Conference item
Link to publisher's version	10.1109/iWAT54881.2022.9811001
Rights	© 2022, IEEE. Personal use of this material is permitted. Permission from IEEE must be obtained for all other uses, in any current or future media, including reprinting/republishing this material for advertising or promotional purposes, creating new collective works, for resale or redistribution to servers or lists, or reuse of any copyrighted component of this work in other works.
Download date	2026-09-25 00:37:28
Item downloaded from	https://hdl.handle.net/10468/13339

2022 International Workshop on Antenna Technology (iWAT) | 978-1-6654-9449-6/22/$31.00 ©2022 IEEE | DOI: 10.1109/iWAT54881.2022.9811001

Flexible and Semi-transparent Chipless RFID Tag based on PDMS-Conductive Fabric Composite

Nadeem Rather
Wireless Sensor Network Group
Tyndall National Institute
Cork, Ireland
nadeem.rather@tyndall.ie

Roy B. V. B. Simorangkir
Wireless Sensor Network Group
Tyndall National Institute
Cork, Ireland
roy.simorangkir@ieee.org

John Buckley
Wireless Sensor Network Group
Tyndall National Institute
Cork, Ireland
john.buckley@tyndall.ie

Brendan O'Flynn
Wireless Sensor Network Group
Tyndall National Institute
Cork, Ireland
brendan.oflynn@tyndall.ie

***Abstract*—This paper presents a 6-bit 25 mm×25 mm×0.4 mm chipless RFID tag based on square ring resonators. The tag is designed and developed using polydimethylsiloxane (PDMS) and conductive fabric composite, resulting in a flexible, semi-transparent, and biocompatible chipless RFID tag, which is suitable for the unobtrusive modern wireless identification and monitoring systems. The tag data is decoded using the monostatic Radar Cross Section method. The tag design is validated with free-space measurements showing a good agreement with simulated results.**

***Index Terms*—chipless RFID, PDMS, ring resonator, radar cross section**

I. Introduction

Radio-Frequency Identification (RFID) is a rapidly growing wireless technology used for the identification and monitoring of people, animals, goods and products [1]–[4]. A classical RFID system is comprised of a single reader (interrogator) and one or multiple tags (transponders). The 'tag' component in the RFID system represents the data-carrying device attached to the items required for identification, tracking and/or monitoring. The 'reader' is used to wirelessly read and/or write the data on the tag using electromagnetic (EM) waves [2]. The reader initiates wireless communications between the reader and tag(s) by emitting EM waves towards the tag. The reflected waves from the tag are then received by the reader which interprets the information encoded in the EM wave. Depending on the method by which the tags are powered, RFID tags fall into two broad categories: active or passive. Active RFID tags have their own power source, which is typically an on-board battery; whereas passive tags are powered entirely using the reader's EM signal [2].

Passive RFID can be broadly categorised into classical chip-based RFID and Chipless RFID (CRFID) [5]. The primary distinction is that with a classical RFID tag, data modulation, data storage, and sensor integration are performed on-chip. A CRFID tag, on the other hand, operates without a chip or battery.

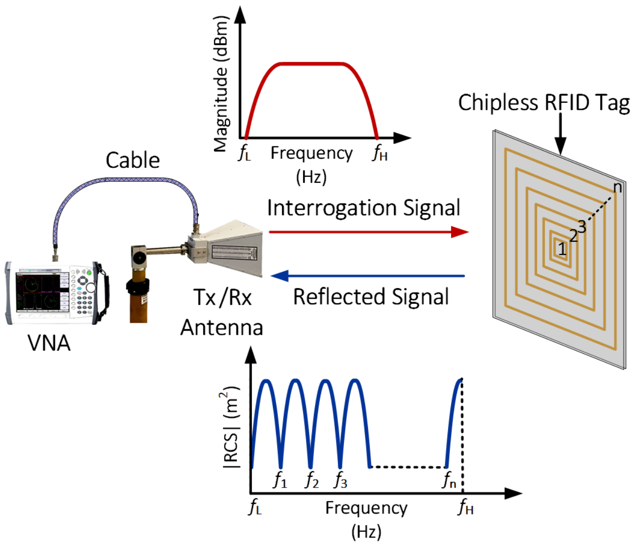

Fig. 1. Basic operating principle of RCS-based CRFID system.

The data encoding is accomplished through variation of the structural properties of the tag, which control the resonant properties of the tag, resulting in a mechanism for passive data encryption in the backscattered EM waves [6]. The extraction of encoded information on the tag relies entirely on data processing techniques employed at the reader (Fig. 1). The ability to implement chipless RFID has proven advantageous in a variety of applications that require low-cost, robust and fully-printable identification and sensing tags [5], [7]. The absence of chip, battery, and other electronics provides CRFID tags with added versatility in harsh and dynamic environments. Current research efforts in this area include the development of flexible or stretchable CRFID tags [7]–[9]. Compared to traditional rigid CRFID tags, the flexible/stretchable tags would benefit from their flexible deployment on the system platforms, independent of the shape of the surface, optimum use of limited spaces, and the users' comfort. This can therefore maximize the potential applications of CRFID, especially with the emerging revolutionary concept of Wireless Body Area Network (WBAN) and Internet of Things (IoT).

In this paper we study the feasibility of using polydimethylsiloxane (PDMS)-conductive fabric composite recently presented in [10] to create a thin, light-weight, flexible, and semi-transparent CRFID tags. This composite has been demonstrated as an excellent option for the construction of flexible antennas, displaying exceptional flexibility, resilience, biocompatibility, and simplicity of manufacturing, compared to other materials typically used for this purpose [11]. For this reason, this composite was chosen to realize the proposed antenna.

The proposed CRFID tag design is based on closed-loop square ring resonator (SRR) approach [12]. The tag is encoded through the variation of RCS response of backscattered signals, which is one of the well-known frequency-domain CRFID encoding techniques [13]–[15] . The presence and absence of the tag resonators is utilized to vary the RCS magnitude within the target spectrum. The design, fabrication, and characterization of the developed tag is presented in this paper.

II. Proposed CRFID Tag

A. Tag Design

The CRFID tag design is shown in Fig. 2. A 6-bit encoding capacity is achieved using the closed-loop Square Ring Resonator (SRR) approach [12] on a compact size of 25 mm×25 mm×0.4 mm. In free space, the perimeter of a closed SRR is equal to the ring's resonant wavelength (λ_0) [12]. A nested configuration is used in the final design to improve the encoding capacity without increasing the tag size. The tag benefits from the SRR symmetrical configuration which allows it to be excited with vertical or horizontal polarisation [15]. The ultra-wide frequency band (UWB) of 3.1 to 10.6 GHz is employed to encode the identification information, as discussed in the literature [5]. CST Microwave Studio 2020 software [16] was used to design and optimize the tag.

To encode the data bits, the RCS minima are used to represent the bit '1'; whereas the absence of its minima, which is associated with the missing ring, is used to represent bit '0' [13]. To demonstrate this, two CRFID tags are developed: one tag with the rings (b_1 to b_6) present to encode '111111' and another tag with two rings (b_1 and b_3) missing to encode '010111'. Fig. 3 (a) and (b) show the topology of both tags. The calculated RCS responses of both tags are shown in (Fig. 3c). The RCS results reveal that removing the rings b_1 and b_3 removes the two of associated minima, validating the above-mentioned encoding mechanism.

B. Materials and Prototype

Nickel-copper coated ripstop from Less EMF Inc. having a thickness of 0.08 mm is used to realize the conductive part

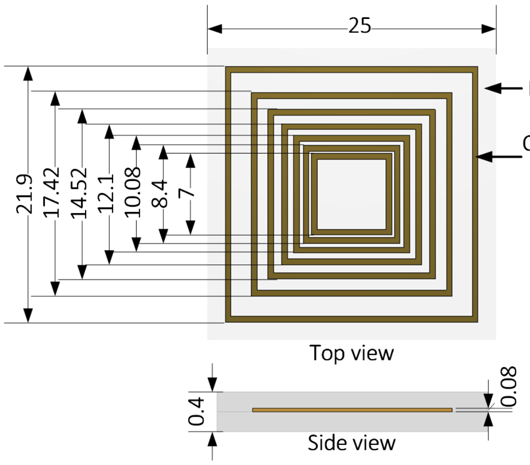

Fig. 2. A 6-bit SRR-based CRFID Tag design.

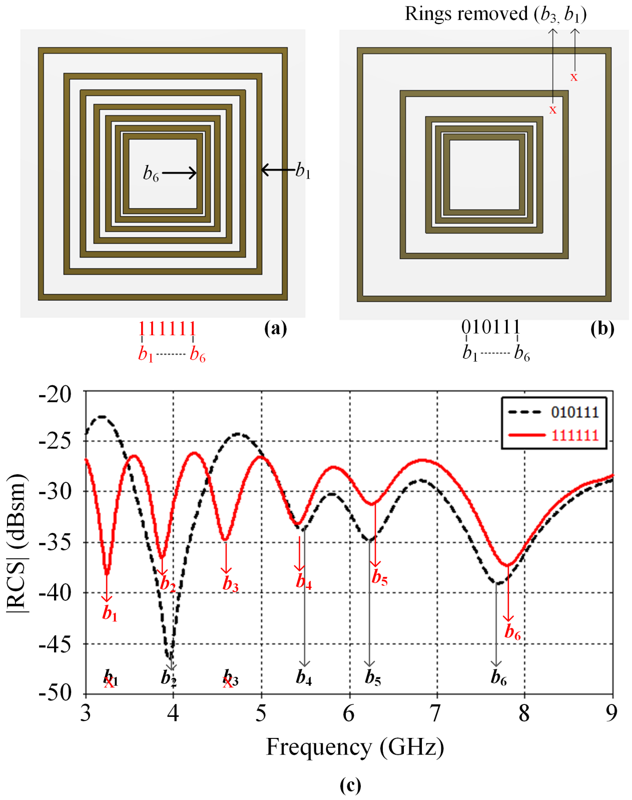

Fig. 3. CRFID tag designs for (a) Tag-1 ('111111') and (b) Tag-2 ('010111'), along with their associated (c) simulated RCS magnitude response.

of the tag. This conductive fabric is then embedded inside a 0.4 mm thick PDMS layer.

It is worth noting that PDMS initial liquid state provides a lot of freedom in obtaining the overall thickness of the tag to achieve the desirable mechanical compatibility of the target applications.

In simulation, PDMS was modelled with a relatively constant permittivity (ε_r) of 2.77 and frequency-dependent loss tangent (tan δ) ranging from 0.02 to 0.076, all based on the measured value at the target operating frequency as

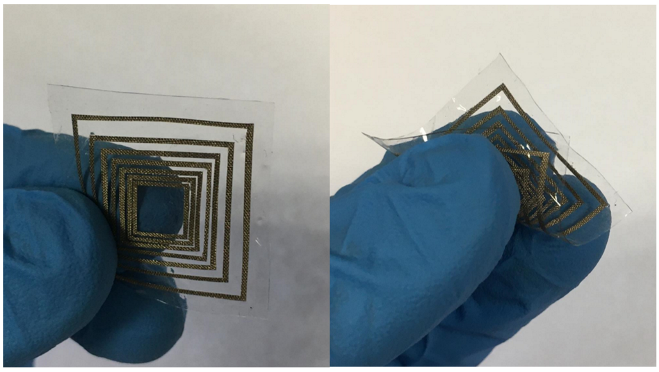

Fig. 4. Fabricated CRFID tag prototype.

reported in [10]. The fabrication of the tag was done through a layer-by-layer assembly process demonstrated in [10]. Fig. 4 shows the photo of the fabricated prototype demonstrating its semi-transparency and high flexibility.

III. Measurements and Results

The RCS measurements of the developed tag was carried out using a monostatic measurement method for its simplicity process. The measurement setup is shown in Fig. 5. A linearly polarized horn antenna (Schwarzbeck BBHA9120D [17]), was connected to a vector network analyzer (VNA), Anritsu MS2038C [18]. A separation distance of 140 mm was kept between the horn and the target tag that was attached flatly on a supporting foam. The measurements were conducted in a closed laboratory room with RF absorbers placed behind the tag to reduce unwanted signal reflections from the surrounding environment. The VNA was used to generate a frequency sweep of 3.1 to 10.6 GHz with 0 dBm power, and to record the input reflection coefficient (S_{11}). The calibration method derived from [15] was used to calculate the RCS from the measured S_{11} (eq. 1).

$$RCS(\sigma) = \left| \frac{S_{11Tag} - S_{11Iso}}{S_{11Ref} - S_{11Iso}} \right|^2 \times \sigma_{Ref} \qquad (1)$$

A. Measurement Procedure

Firstly, the measurement with all the structures in place except the tag was undertaken and S_{11Iso} was recorded. Secondly, the measurement with a square flat copper plate (25 mm$\times$25 mm) as a reference calibration object was done to get S_{11Ref}. Finally, the tag under test was placed and the measurement of S_{11Tag} was taken.

The known RCS of the reference flat metal plate for calibration σ_{Ref} was calculated using equation (2) below,

$$RCS(\sigma_{Ref}) = 4\pi A^2/\lambda^2 \quad m^2 \qquad (2)$$

where A = area, π = 3.14, and λ = wavelength.

B. Results

The simulated and measured RCS results of both tags are compared in Fig. 6. In general, a good agreement between the simulated and measured results is observed.

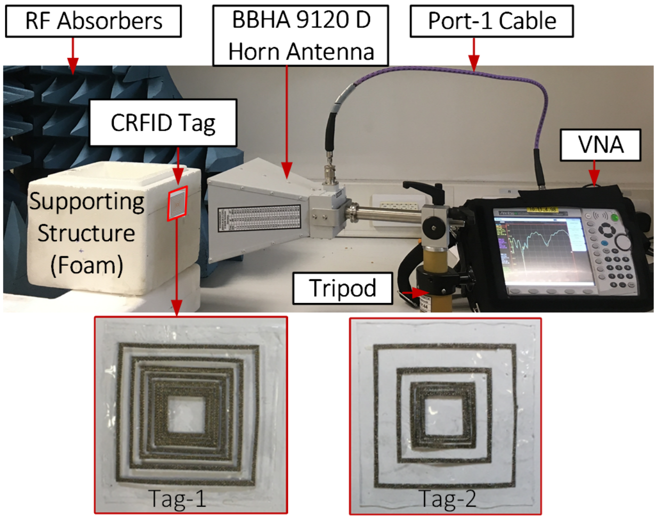

Fig. 5. Free-space monostatic RCS measurement setup.

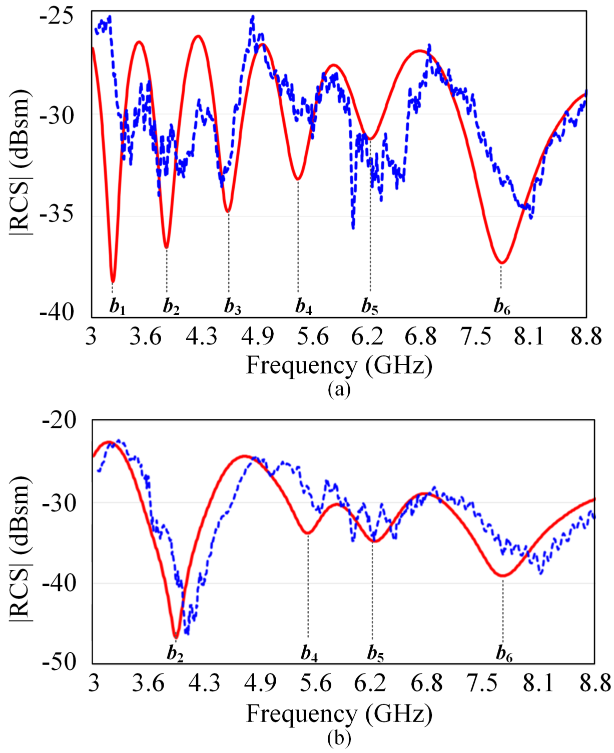

Fig. 6. Free-space RCS simulation and measured responses: (a) Tag-1, (b) Tag-2.

Some discrepancies in the results (e.g., the shift in the minima locations and the difference in the RCS peak) are most likely attributed to fabrication tolerances. Nevertheless, the RCS responses of both tags are still readily identifiable.

IV. Conclusion

This paper presents an SRR based, 6-bit CRFID tag that is implemented using PDMS and conductive fabric. The materials are used to prove its feasibility for the development of thin, flexible, and unobtrusive CRFID tag, potential for various modern wireless communication and sensing applications, including WBAN and IoT. Tag data are encoded using RCS techniques with the presence of minima representing a logic '1' and their absence representing a logic '0'. A monostatic RCS measurement using one linearly polarized antenna provides accurate results for decoding encoded information from the tags. Future work will add a sensing capability to the developed tag and will also optimize the tag design for a specific application, for instance, human-centric identification and sensing, which involve very lossy human body tissue as an operating environment.

ACKNOWLEDGMENT

This paper has emanated from research funding provided by Science Foundation Ireland (SFI) as part of the SFI Centre VistaMilk (SFI 16/RC/3835). Aspects of this work have been supported under the following Grant Numbers: Connect Centre for Future Networks and Communications (13/RC/2077), The Insight Centre for Data Analytics (SFI/12/RC/2289) as well as the Enterprise Ireland funded Holistics DTIF (EI-DT20180291-A). All work is co-funded under the European Regional Development Fund.

REFERENCES

[1] E. Perret, *Radio frequency identification and sensors: from RFID to chipless RFID*. John Wiley & Sons, 2014.

[2] K. Finkenzeller, *RFID handbook: fundamentals and applications in contactless smart cards, radio frequency identification and near-field communication*. John wiley & sons, 2010.

[3] M. Pigeon, N. Rather, B. O'Flynn, and J. Buckley, "Nfc sensing of tear fluid for animal health monitoring," in *2021 15th European Conference on Antennas and Propagation (EuCAP)*. IEEE, 2021, pp. 1–5.

[4] D. R. Gawade, J. Buckley, N. N. Rather, S. Ziemann, A. Zabeo, J. Barton, D. Iacopino, K. Schuhmann, M. Anders, M. Burke *et al.*, "A battery-less nfc sensor transponder for museum artefact monitoring-a review of nfc sensor technology and a proposed solution," 2019.

[5] S. Preradovic and N. C. Karmakar, "Chipless rfid: Bar code of the future," *IEEE microwave magazine*, vol. 11, no. 7, pp. 87–97, 2010.

[6] R. Rezaiesarlak and M. Manteghi, *CHIPLESS RFID*. Springer, 2016.

[7] S. K. Behera, "Chipless rfid sensors for wearable applications: A review," *IEEE Sensors Journal*, 2021.

[8] A. Vena, E. Moradi, K. Koski, A. A. Babar, L. Sydänheimo, L. Ukkonen, and M. M. Tentzeris, "Design and realization of stretchable sewn chipless rfid tags and sensors for wearable applications," in *2013 IEEE International Conference on RFID (RFID)*. IEEE, 2013, pp. 176–183.

[9] A. Ramos, Z. Ali, A. Vena, M. Garbati, and E. Perret, "Single-layer, flexible, and depolarizing chipless rfid tags," *IEEE Access*, vol. 8, pp. 72 929–72 941, 2020.

[10] R. B. Simorangkir, Y. Yang, R. M. Hashmi, T. Björninen, K. P. Esselle, and L. Ukkonen, "Polydimethylsiloxane-embedded conductive fabric: Characterization and application for realization of robust passive and active flexible wearable antennas," *IEEE Access*, vol. 6, pp. 48 102–48 112, 2018.

[11] B. Mohamadzade, R. M. Hashmi, R. B. Simorangkir, R. Gharaei, S. Ur Rehman, and Q. H. Abbasi, "Recent advances in fabrication methods for flexible antennas in wearable devices: State of the art," *Sensors*, vol. 19, no. 10, p. 2312, 2019.

[12] C. A. Balanis, *Antenna theory: analysis and design*. John wiley & sons, 2015.

[13] N. C. Karmaker, "Tag, you're it radar cross section of chipless rfid tags," *IEEE Microwave Magazine*, vol. 17, no. 7, pp. 64–74, 2016.

[14] M. Polivka, J. Havlicek, M. Svanda, and J. Machac, "Improvement of rcs response of u-shaped strip-based chipless rfid tags," in *2015 European Microwave Conference (EuMC)*. IEEE, 2015, pp. 107–110.

[15] A. Vena, E. Perret, and S. Tedjini, "High-capacity chipless rfid tag insensitive to the polarization," *IEEE Transactions on Antennas and Propagation*, vol. 60, no. 10, pp. 4509–4515, 2012.

[16] CST. CST studio suite electromagnetic field simulation software. [Online]. Available: https://www.3ds.com/products-services/simulia/products/cst-studio-suite/

[17] Schwarzbeck. (1999) BBHA 9120 D kernel description. [Online]. Available: http://http://www.schwarzbeck.de/Datenblatt/k9120d.pdf

[18] Anritsu. Anritsu VNA master and spectrum analyzer. [Online]. Available: https://www.anritsu.com/en-us/test-measurement/products/ms2038c